One Pot Green Synthesized Silver Nanoparticles as a Selective Sensor for Hg2+ Ions.

Nasir Mahmood Abbasi (nasir343@zju.edu.cn)
Shenzhen University https://orcid.org/0000-0001-9256-2251
Najma Nasim
Women University
Sana Khan
Women University
Farid Ahmad
Institute for advanced study Shenzhen university
Usman Hameed
Women University

Research Article

Keywords: Green synthesis, Nanotechnology, Silver Nanoparticles, Surface plasmon resonance, calorimetric detection, and tap water.

Posted Date: July 14th, 2021

DOI: https://doi.org/10.21203/rs.3.rs-706124/v1

One pot green synthesized silver nanoparticles as a selective sensor for Hg^{2+} Ions.

Nasir Mahmood Abbasi*[a], Najma Nasim[c], Sana Khan[c], Farid Ahmed*[b] , Usman Hameed[c]

[a] College of Physics and Optoelectronic Engineering, College of Materials Science and Engineering, Institute of Microscale Optoelectronics, Collaborative Innovation Centre for Optoelectronic Science & Technology, Key Laboratory of Optoelectronic Devices and Systems of Ministry of Education and Guangdong Province, Shenzhen Key Laboratory of Micro-Nano Photonic Information Technology, Guangdong Laboratory of Artificial Intelligence and Digital Economy (SZ), Shenzhen University, Shenzhen 518060, P.R. China

*[b] Institute for advanced study Shenzhen university

[c]Department of Chemistry, Women University of Azad Jammu@ Kashmir Bagh-Pakistan

ABSTRACT: The domains of science and technology, especially environmental protection, have brought a lot of change in nanotechnology. In the modern period, the growth of animals and plants with enough quantities is fundamentally obligatory by heavy metal ions (M^{+}), such as $Cr^{3+,}$ Zn2+, $Ni^{2+,}$ Cu^{2+} and $Hg^{2+.}$. However, because of their presence in both human and animal food webs, these metal ions are toxic to living things at relatively high concentrations. The ecologically friendly green approach was utilized to synthesis starch functionalized silver nanoparticles (St-Ag NPs) using water as a solvent, starch as a stabilizing agent, and glucose as a reducing agent. KOH has been used as an activator for glucose activation. The influence of diverse solutions such as AgNO3, starch, glucose, and KOH on the production of St-AgNPs was investigated. To see how these substances affect the production of St-Ag NPs, different controlled reactions were carried out in the absence of starch, glucose, and KOH. Starch, glucose, and KOH are discovered to play important roles in the synthesis of AgNPs. UV-Vis absorption spectroscopy, Fourier transform infrared (FT-IR), X-ray diffraction (XRD), and scanning electron microscope (SEM) were used for the characterization of St-Ag NPs. These starch functionalized AgNPs were used for the detection of heavy metals at 25℃. It is found during the screening process only Hg^{2+} showed clear changes in the color and absorption intensity of AgNPs which may be due to redox reaction that can occur between Ag^{0} and Hg^{2+}. On the other hand, the color and absorption intensity of nanoparticles remain unchanged in the presence of all the other tested metals ion. The presence of other metal ions was also tested in the system. The proposed method has strong selectivity and sensitivity to Hg^{2+} ions. Using UV-visible spectrophotometry, the method produced had a detection limit of 1ppm. The proposed method for detecting Hg^{2+} in tap water samples was found to be successful..

Keywords: Green synthesis, Nanotechnology, Silver Nanoparticles, Surface plasmon resonance, calorimetric detection, and tap water.

* Correspondence to Dr. Nasir Mahmood Abbasi, E-mail: nasir343@zju.edu.cn and Dr Farid Ahmad, Email farids_ahmed@yahoo.com Tel:+86-13699819774 Fax:

1 Introduction

During the last decade, the emerging field of plasmonic-based nanotechnology brought a revolutionary track in the discipline of applied sciences and has many practical applications of nanoparticles in the field of environmental sciences such as wastewater treatment. Heavy metal ions (M^+), such as Cr^{3+}, Zn^{2+}, Ni^{2+}, Cu^{2+}, and Hg^{2+} are essentially mandatory for the growth process of both animals and plants at appropriate concentrations. However, these metal ions are harmful to living creatures at relatively high concentrations because of their addition in both human and animal via biological food webs [1, 2].

Mercury ion (Hg^{2+}), which is widely distributed in the atmosphere, soil on the earth's surface, and even in water, and, is one of the most lethal and hazardous metal pollutants [3, 4]. There are various sources of mercury such as the burning of coal in power plants, natural liberation of gases from earth surface during vulcanization, etc., and metals extraction process[5]. Hg^{2+} is a persistent pollutant because naturally, it cannot decompose in the environment[6]. In water, fishes consume mercury as it is dissolved in water and through the food web, this is the major way of mercury accumulation in humans[7]. It can damage the brain, nervous system, and immune system [4].

Therefore, detection of poisonous metals in the aquatic environment and biological system has become a crucial need of the present-day world[8]. During last decade various methods have been developed for Hg^{2+} detection including electrochemical methods [9], optical detections[10], atomic absorption spectroscopy, inductively coupled plasma mass spectroscopy [11] and fluorescent spectroscopy [12]. However, most of these procedures are inconvenient because they use complicated instruments, painstaking, and are time-consuming [13]. Therefore, the introduction of a logical technique that is not just too easy and cheap but also useful and reproducible able to sense the toxic metal pollutants in the ecological samples is greatly needed.

For these mentioned problems, approaches for low cost and rapid detection in the mercury environment using silver nanoparticles (AgNPs) or golden nanoparticles are advantageous (AuNPs).

Synthesizing metallic nanoparticles(AgNPs and AuNPs) in an environmentally friendly manner is a key step in nanotechnology. In the field of selective and sensitive detection methods, the use of environmentally friendly nanotechnology has recently become increasingly significant. [25, 26]During the last decade, Colorimetric sensors, in particular, have a distinct advantage because of their versatility, rapidity, high selectivity, and ease of use, which includes the ability to perform real-time qualitati[25]ve and quantitative analysis.[27, 28]

Nanotechnology has the potential to boost life sciences, healthcare, and industrial technology significantly. For example, Lax man et al. [16]presented an optical process for careful recognition of Hg^{2+} depending upon the aggregation of AgNPs. Jing Wang et al. reported a highly sensitive method for sensing Hg^{2+}, ascorbic acid, and Cd^{2+} by using trithiocyanuric acid gold NPs[17]. Senapati and co-workers in their work showed the use of tryptophan coated gold nanoparticles for selective and efficient detection of Hg^{2+}[18]. Chai et al. presented colorimetric detection of Pb^{2+} using glutathione functionalized AuNPs[19]. But, these approaches typically use some chemicals as reducing agents that frequently produce toxic side products[20]. Some of them used organic reagents as the functional selective reagents, which are unstable and easily oxidized. While some tagging agents costly to use these techniques as sensors for real life [21]. As well as the production processes of nanoparticles used in sensing systems are complex [22]. These sensors are generally derivatives of fluorescent dyes, usually harmful to the environment [23, 24].

. Nowadays, apparent detection by using AuNPs and AgNPs is a common practice because of color changes which are simply viewed with naked eyes instead of complicated instruments[14]. These nanoparticles are used as colorimetric probes for sensing lethal metal ions

from ecological samples via cheap and simple procedures[15] Two basic reasons, makes the AgNPs as a selective candidate for the sensing process of Hg^{2+} instead of AuNPs: First, AgNPs have a high extinguishing value of AuNPs. Second AgNPs can also be oxidized by Hg^{2+} which causes color change and decrease in the UV-visible UV spectrum absorption of the AgNPs. The use of silver nitrate that was lowered by D-glucose in the presence of starch synthesizes AgNPs. D-Glucose is an ecologically favorable and mild reducing agent, which is activated in the presence of a basic catalyst. Starch, act as a protecting agent as it contains many hydroxyl (-OH) groups that will simply attach to the surface of AgNPs through the Ag-O bond and prevent the accumulation of AgNPs [29]. The starch and D-glucose are biomolecules that are, non-toxic and biocompatible.

In this article we propose, a novel, fast and very selective detection method for various heavy metals by using starch-functionalized AgNPs, with a green synthesis approach. The selectivity of this detection system of Hg^{2+} by using starch stabilized AgNPs is outstanding when we compare them with other noble metal ions, like Pb^{2+}, Al^{3+}, Zn^{2+}, Cu^{2+}, $Fe^{3+,}$ and detection of Hg^{2+} can be carried out even in the presence of a mixture of the various heavy metal ions.

2 Materials and Methods

2.1 Chemicals

$AgNO_3$, KOH, KCl, NaCl, $FeCl_3$, $ZnCl_2$, $HgCl_2$, $NiCl_2.6H_2O$, $CuSO_4$, $AlCl_3$ were purchased from Sigma Aldrich. D-glucose and soluble starch ($(C_6H_{10}O_5)_n$) were also purchased from Sigma Aldrich. Distilled water was used during the research. All of the required substances were received in pure form so there was no need for additional purification.

2.2 Synthesis of starch-stabilized AgNPs

In a typical synthetic procedure, 2 mL of D-glucose (0.1 M), 2 mL of starch (0.2 wt %) and 0.02 mL of KOH (0.1 M) were added into 5 mL of $AgNO_3$ (10 mM). After that, the mixture was heated at 30 °C for 10 min with continuous stirring at (100 rpm). After that formation of AgNPs was indicated by a color change from colorless to deep Reddish yellow. The basic steps involved during the synthesis process are mentioned in Scheme 1. These nanoparticles dispersion was centrifuged at 1200 rpm to obtain solid particles. Finally, the prepared nanoparticles were stored at 25 °C for further characterization.

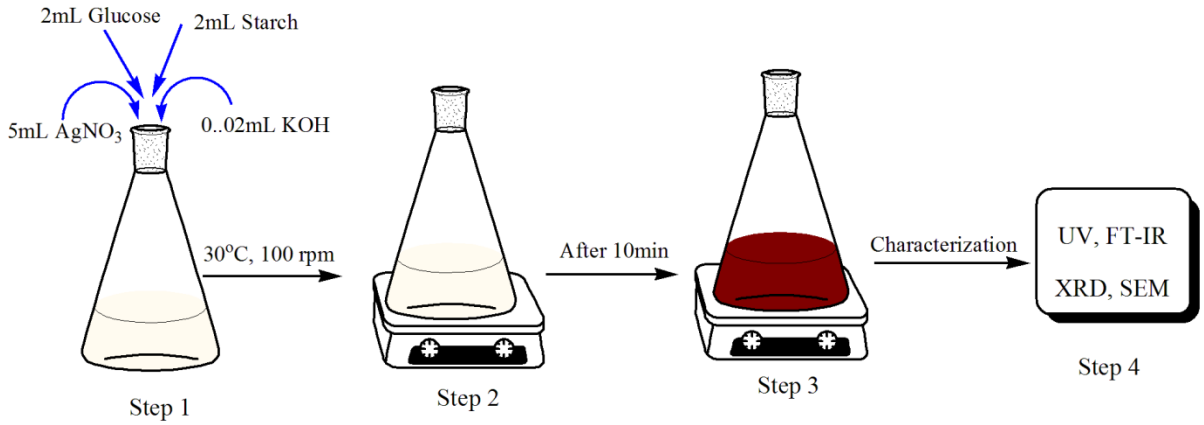

Scheme 1: Different Steps involved during the preparation of AgNPs

2.3 Characterization

The synthesized AgNPs were analyzed first by UV-vis spectrophotometer. UV-vis absorption studies were done by using UV-1800 double beam spectrophotometer (Shimadzu, Japan), utilizing quartz cuvettes of 1.0 cm path length in the UV range from 200 – 800 nm.XRD was recorded on a Bruker D-8 powder X-ray diffractometer by Cu-K radiation (λ = 0.15418 nm) over a range of 20°–90°with a step size of 0.02°. FT-IR spectra were obtained by using FT-IR 8400Schimadzu using KBr disk (4000-400 cm^{-1}).

2.4 General procedure for the calorimetric determination of Hg^{2+}

For detection of Hg^{2+} using AgNPs dispersion, 1 mL (100 ppm) of aqueous solutions of $Pb^{2+,}$ $Cu^{2+,}$$Al^{3+}$, Zn^{2+}, Fe^{2+}, Ni^{2+} and Hg^{2+} were added respectively into 1 mL of AgNPs

dispersion. To find out the detection limit various concentrations of $HgCl_2$ (1-100ppm) were prepared from the stock solution by quantitative dilution. Keeping the total volume of mixture constant (2 mL), an equal volume of Ag-NPs and $HgCl_2$ (each concentration.) were mixed. To check out the selectivity of the detection system 100 ppm aqueous solutions of Pb^{2+}, Cu^{2+}, Al^{3+}, Zn^{2+}, Fe^{2+}, $Ni^{2+,}$ and Hg^{2+} were prepared. 1 mL of every solution was added into 1 mL solution of Hg^{2+} (100 ppm) and 1 mL of AgNPs dispersion. All the solution and dilution processes are carried out at room temperature.

To determine the binding stoichiometry of Hg^{2+} and AgNPs, Hg^{2+} (100ppm) solution ratios from 0.1 to 2 mL were mixed with AgNPs dispersion in opposite ratios of volume. To find out the role of pH on the sensing study pH of AgNPs was varied from 1 to 12. To study the practical applications of the planned strategy, we used tap water for Hg^{2+} detection. About 100 ppm Hg^{2+}solution was prepared in tap water, and then1 mL of that dispersion was mixed with AgNPs dispersion in tap water. All of these mixtures were kept at room temperature for 10 minutes to monitor the effect of Hg^{2+} on AgNPs dispersion in tap water.

3 Results and Discussions

3.1 Visual Detection of AgNPs Synthesis

The color of the reaction mixture changed within 10 min from colorless to reddish yellow (as shown in Figure 1 A), after mixing starch, glucose, and KOH solution with $AgNO_3$ solution. Thus, Ag^+ reduction was confirmed as the colorless silver nitrate solution altered to yellowish-brown. It is assumed that the production of AgNPs is a redox reaction where Ag^+ is reduced to Ag^0 with the oxidation of glucose to corresponding gluconic acid that was later on confirmed through FT-IR.

3.2 UV–Visible Absorption Spectroscopy

The synthesized AgNPs were analyzed by UV–visible absorption spectroscopy technique because of the surface Plasmon resonance (SPR) phenomenon. When light waves interact with free electrons present in the reduced AgNPs surface plasmon resonance originate. For confirmation of the formation of AgNPs UV spectra were recorded for a starch solution, D-Glucose solution, and KOH solution, which don't show any characteristic absorption due to the absence of SPR. UV–vis spectrum of the AgNPs suspensions shows an absorption maximum at 430 nm, as shown in Figure 1(A). As a function of synthesis/reaction time, the absorbance was found to increase and a maximum was observed after a reaction time of 10 min. Thus, the optimum reaction time for the synthesis of AgNPs was found to be 10 min. Under the influence of high temperature, the rate of reduction of Ag^+ increases, and therefore the rapid synthesis of AgNPs could be achieved [30].

3.3 X-ray Diffraction

A characteristic XRD pattern of synthesized AgNPs showed various reflections, at 38.2° (111), 44.3◦ (200), and 64.5° (220) as shown in Figure 1(B). These sharp Bragg peaks may be produced due to the stabilization of nanoparticles by starch that acts as a capping agent. The peak related to the (111) plane was more prominent than the rest of the planes, signifying that the (111) plane was the major orientation in the face-centered cubic (fcc) structure of AgNPs.The XRD results of AgNPs are similar with previously reported literature [31].

3.4 FT-IR Analysis

FT-IR spectra were used to recognize the functional groups in a different types of compounds. For comparison, IR spectra were recorded for D-Glucose, starch, and AgNPs. In spectra of D-glucose& starch, there is a wide peak at 3200–3500 cm^{-1}, which reflects the stretching vibration of OH group (i.e. hydrogen-bonded), and a sharp peak at 1725 cm^{-1} represents the C=O stretch of aldehyde group. The sharp peaks at 2900 $cm^{-1}$and 1100 $cm^{-1}$are

the stretching vibrations of aldehyde C-H and C-O, respectively. Moreover, OH bending vibration is reflected in the region of 1433 cm^{-1}. In IR spectra of AgNPs, the peaks of OH group stretching and bending are less intense. While a sharp peak in the region of 1710cm^{-1} appears which indicates the presence of the COOH group as shown in Figure 1(C). Its means that during the formation of AgNPs the C=O and OH groups of Starch and D-Glucose cause the reduction of Ag^{+} ions from $AgNO_3$ and itself oxidized into respective acid. Kumari Jyoti et al. reported similar observations in their work [32].

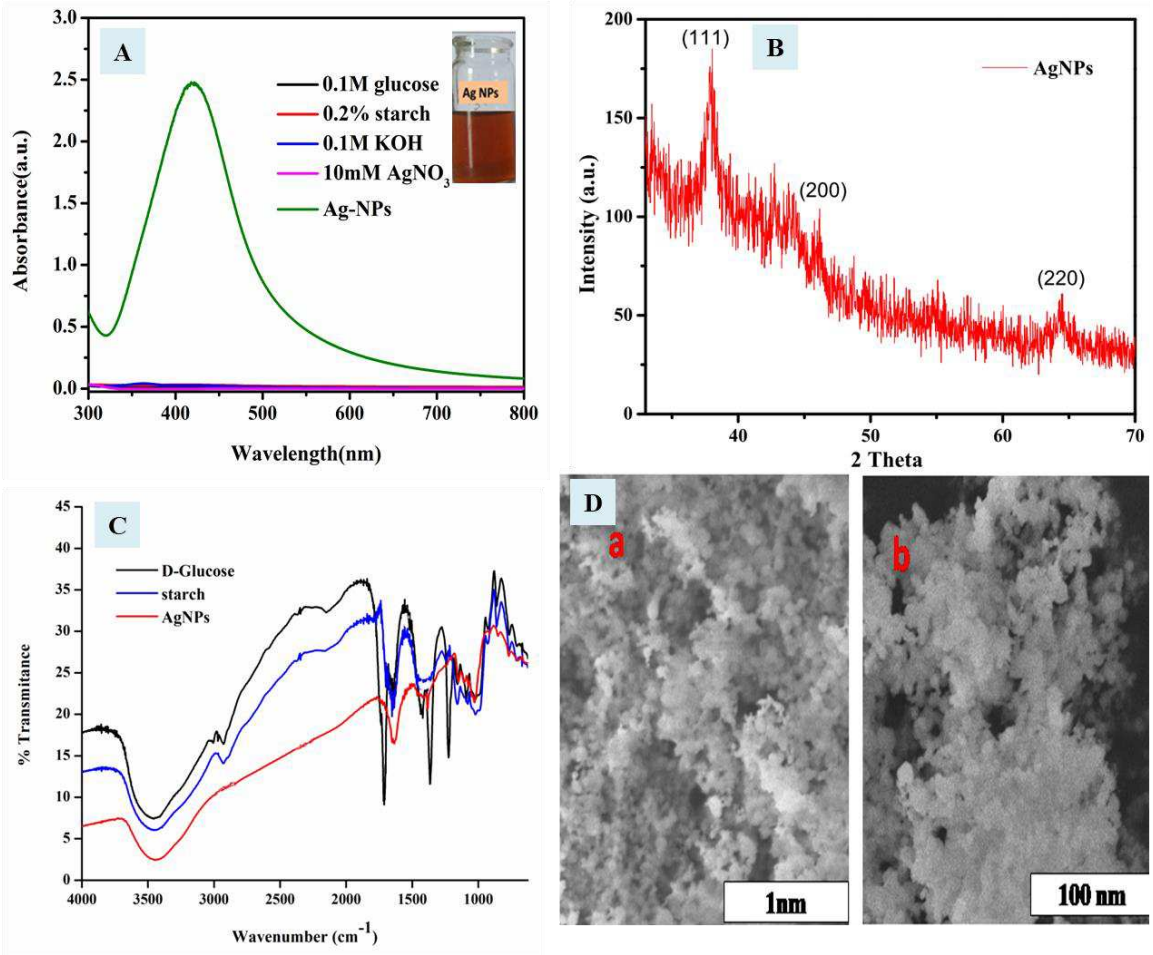

Figure 1 :**(A)** UV spectra show Glucose, Starch, KOH, and $AgNO_3$ and synthesized AgNPs, **(B)**XRD image of synthesized silver nanoparticles. **(C)** FT-IR results show (a) D-glucose (b) starch and (c) synthesized AgNPs.

3.5 Scanning Electron Microscopy

The surface morphology monitored by SEM images reveals various shapes in the form of spherical AgNPs. Figure 1 (D) shows the low and high magnification images of AgNPs. One can observe that the particle size lies in the range of 1-100nm. This may be due to the availability of the different quantities of capping agents during their synthesis process[33].

3.6 Parameter Optimization

The volume of $AgNO_3$ (10 mM) (NN-A1 to NN-A5), starch (0.2%) (NN-A6 to NN-A10), and glucose (0.1M) (NNA-11 to NNA-15) were varied from 1 to 5mL as shown in Table 1. UV spectra show that absorption gradually increases with an increase in the volume ratio of $AgNO_3$ might be due to rising in the rate of redox reaction between $AgNO_3$ and OH groups of starch and glucose. Whereas, absorption gradually decreases with an increase in the volume ratio of starch and glucose (as shown in Figure 2 A, B, C) that is due to a simple dilution effect.

Table 1: Experimental details for different volume ratios of $AgNO_3$, starch, and glucose during the synthesis of Ag-NPs.

Sample No.	$AgNO_3$ (mL)	Starch (mL)	Glucose (mL)	KOH (mL)	Temperature (^{0}C)	Stirring (rpm)	Time (min)
NN-A1	**1**	5	2	0.02	30	100	10
NN-A2	**2**	5	2	0.02	30	100	10
NN-A3	**3**	5	2	0.02	30	100	10
NN-A4	**4**	5	2	0.02	30	100	10
NN-A5	**5**	5	2	0.02	30	100	10
NN-A6	5	**1**	2	0.02	30	100	10
NN-A7	5	**2**	2	0.02	30	100	10
NN-A8	5	**3**	2	0.02	30	100	10
NN-A9	5	**4**	2	0.02	30	100	10
NN-A10	5	**5**	2	0.02	30	100	10
NN-A11	5	2	**1**	0.02	30	100	10
NN-A12	5	2	**2**	0.02	30	100	10
NN-A13	5	2	**3**	0.02	30	100	10
NN-A14	5	2	**4**	0.02	30	100	10
NN-A15	5	2	**5**	0.02	30	100	10

The concentration of $AgNO_3$(NN-A16 to NNA-20) was varied from 2 to 10mM while the concentration of glucose (NNA-21 to NNA-25) starch ((NN-A26 to NN-A30), and KOH (NNA-31 to NNA-35) was varied from 0.1 to 0.5M as shown in Table 2. UV spectra show maximum absorption at 430 nm, which gradually increases with an increase in concern of $AgNO_3$ (as shown in Figure 2 D, E, F). It is expected that a large number of Ag^+ would be available during the redox reaction resulting in a higher yield of AgNPs, which is responsible for the increase in the absorption peak [34].

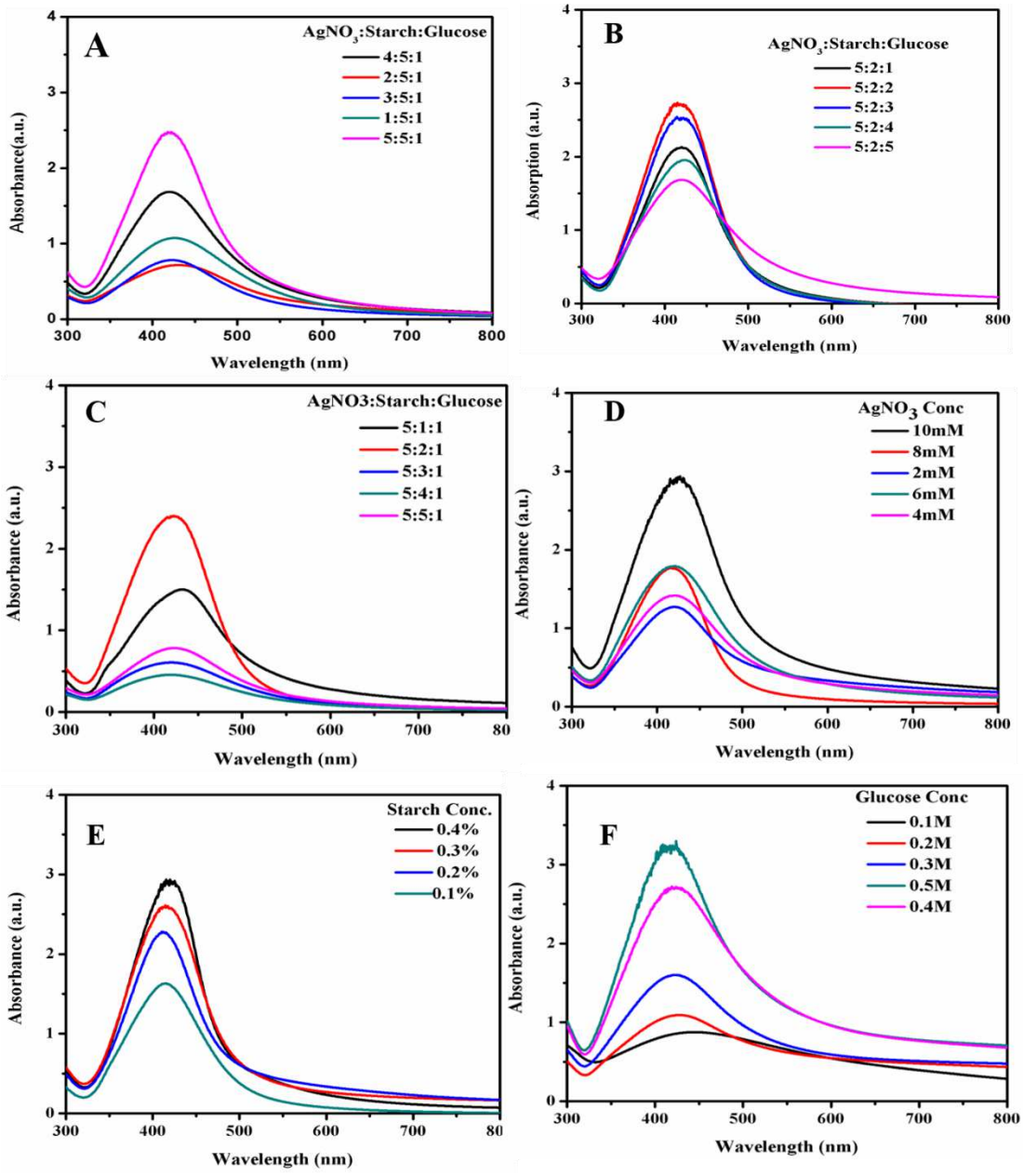

Figure 2 : UV spectrum show AgNPs formation (A) at diverse volume ratios of 10 mM $AgNO_3$ (1 to 5 mL), (B) at different volume ratios of0.1 M glucose, (C) at different volume ratios of0.2 % starch and (D) at 5 mL of different concentration of $AgNO_3$, (E) at 2 mL of various concentrations. of starch, (F) at 2 mL of various concentrations. of glucose.

Similar behavior was observed in UV spectra of starch, glucose, and KOH, absorption at 430 nm gradually increase with an increase in concentrations due to an increase in the rate of nanoparticle synthesis in a highly basic environment and adequate availability of the reducing & stabilizing agent. But in concentrated solutions concentration of OH increases which causes aggregation on surface AgNPs which increases in peak intensity [35],[22].

Table 2: Experimental details for different concentrations. of $AgNO_3$, glucose, starch, and KOH in the synthesis of AgNPs

Sample No	$AgNO_3$ Conc. (mM)	Starch Conc. (%)	Glucose Conc. (M)	KOH Conc. (M)	Time (min)	Temp (^{0}C)	Stirring (rpm)
NN-A16	**10**	0.2	0.1	0.1	10	30	100
NN-A17	**2**	0.2	0.1	0.1	10	30	100
NN-A18	**4**	0.2	0.1	0.1	10	30	100
NN-A19	**6**	0.2	0.1	0.1	10	30	100
NN-A20	**8**	0.2	0.1	0.1	10	30	100
NN-A21	10	0.2	**0.1**	0.1	10	30	100
NN-A22	10	0.2	**0.2**	0.1	10	30	100
NN-A23	10	0.2	**0.3**	0.1	10	30	100
NN-A24	10	0.2	**0.4**	0.1	10	30	100
NN-A25	10	0.2	**0.5**	0.1	10	30	100
NN-A26	10	**0.1**	0.1	0.1	10	30	100
NN-A27	10	**0.2**	0.1	0.1	10	30	100
NN-A28	10	**0.3**	0.1	0.1	10	30	100
NN-A29	10	**0.4**	0.1	0.1	10	30	100
NN-A30	10	**0.5**	0.1	0.1	10	30	100
NN-A31	10	0.2	0.1	**0.1**	10	30	100
NN-A32	10	0.2	0.1	**0.2**	10	30	100
NN-A33	10	0.2	0.1	**0.3**	10	30	100
NN-A34	10	0.2	0.1	**0.4**	10	30	100
NN-A35	10	0.2	0.1	**0.5**	10	30	100

A controlled experiment without glucose and starch was carried out. UV spectrum shows that in the absence of glucose & starch absorption at 430 nm is minimum (as shown in Figure 3 B, C). That might be due to a slight reduction of Ag^{+} to Ag^{0} in the absence of glucose that acts as a reducing agent. Whereas starch act as a stabilizing agent and in the absence of starch AgNPs are unstable and get aggregated which results in a decrease in surface plasmon resonance peak [29].

AgNPs can form even in the absence of KOH & UV spectra reveals that absorption of AgNPs gradually increases (as given in Figure 3D) with a raise in heating time in the absence of KOH. It can be concluded that in the absence of base pH of the reaction mixture was low hence the rate of reduction of $AgNO_3$ to AgNPs was time-consuming[36].

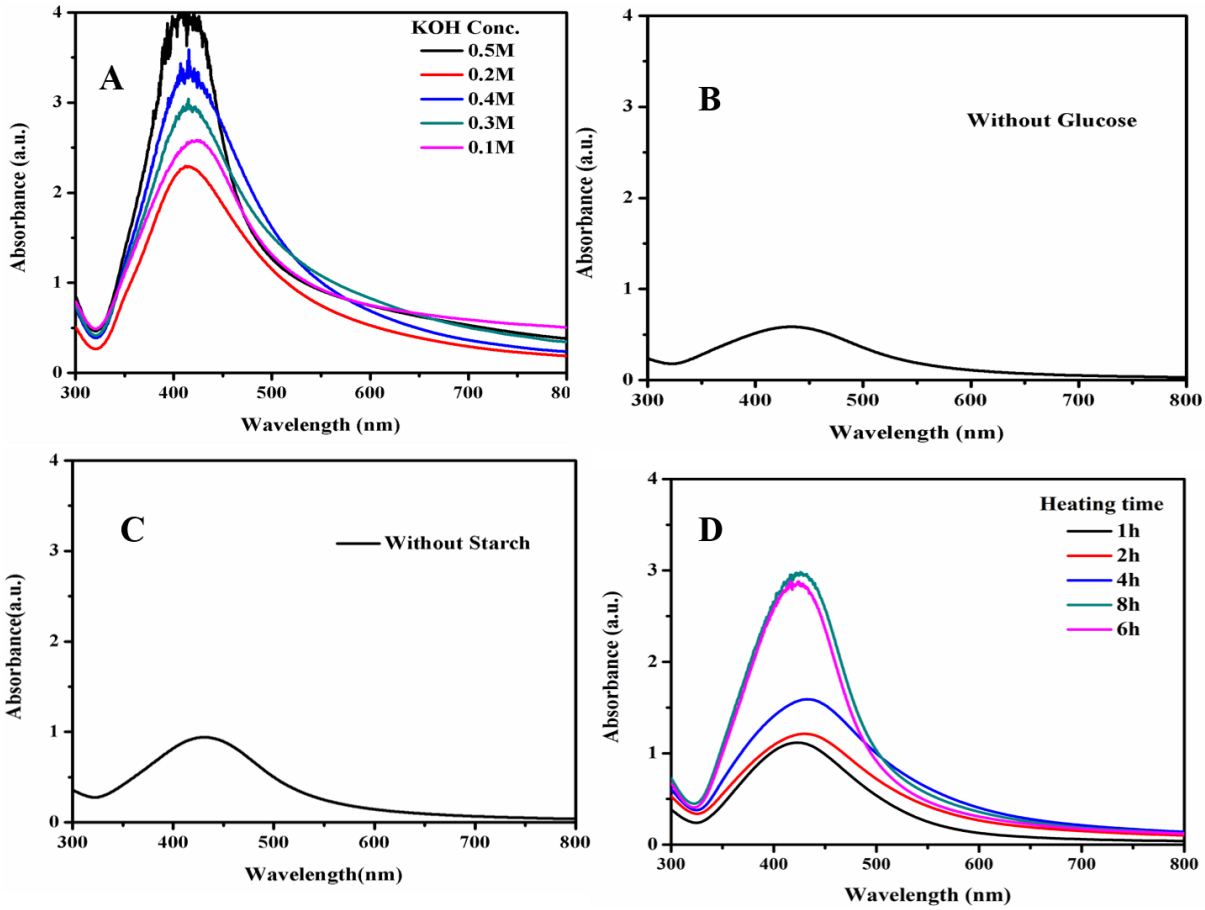

Figure 3: UV spectrum shows AgNPs formation, (A) at 0.02 mL of different concentrations of KOH, (B) without 2mL of glucose, (C) without 2 mL of starch, (D) without 0.02 mL of KOH.

3.7 Possible mechanism of the formation of silver nanoparticle:

This reaction, an example of hydrolysis of starch, catalyzed by base (KOH) giving simpler molecules, like glucose. Glucose is used as a reducing agent for silver nitrate to silver metal. During the reactive aldehyde group of glucose reduce Ag^{+} to Ag^{o} and itself oxidized to gluconic acid (as shown in Scheme 3), while the starch stabilized the silver nanoparticles.

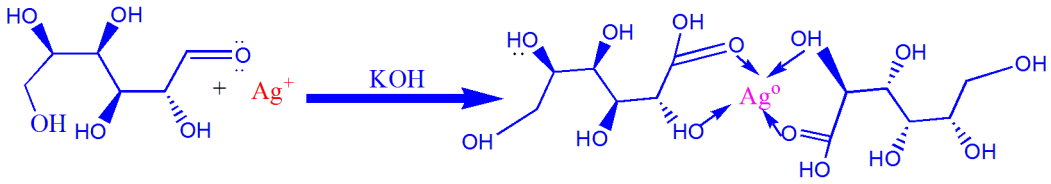

Scheme 2: Possible route for the synthesis of AgNPs.

3.8 Calorimetric determination of Hg^{2+}

AgNPs have shown their potential in visual as well as SPR detection-based sensing of heavy metals. Here AgNPs were used for sensing Hg^{2+} in water. The decolorization of AgNPs and decrease in their UV absorption peak intensity is due to the redox reaction that caused the aggregation of the nanoparticles. During the reaction Ag^{0} from AgNPs is oxidized to Ag^{+} while Hg^{2+} is reduced to Hg^{0} as the typical electrode potential value of (Hg^{2+}/Hg (E_0 = 0.85 V) and Ag^{+}/Ag (E_0 = 0.79 V). Furthermore, because Hg^{2+} has a greater reduction potential than Ag+, the redox reaction $2Ag + 2Hg^{2+} = 2Ag^{+} + Hg^{2+}$ occurs spontaneously. As illustrated for the original colorless solution $AgNO_3$, oxidizing Ag(0) to Ag^{+} changes the color of AgNPs from yellowish brown to colourless (Scheme 3):. The colorimetric detection of mercury by AgNPs is based on this redox process. Ag(0) AgNPs to Ag^{+} cannot oxidize the bulk of transition metals, alkaline, and alkaline earth metals due to their lower potential than Ag+, allowing for extremely selective Hg^{2+} analyses.Thus, the oxidation of AgNPs leads to the loss of its characteristic color and a decrease in its UV absorption peak intensity.

This revised mechanism promotes the mechanisms previously proposed.[37-40] However, after addition of Hg ions, some colorimetric mercury detection methods with various surfactant or functional AgNP's might yield a colored mixture that would suggest a distinct reaction mechanism.It is found that the role of surfactant is very important during the sensing process [41]Instead of a direct reaction between Hg^{2+} ions and Ag(0) of AgNPs, the interaction between Hg ions and capping agents to form larger nanoparticles that lead to aggregation plays a larger role in these reactions. The interaction of Hg^{2+} ions and Ag(0) of AgNPs in the presence of Starch as a surfactant is shown in Scheme 4.

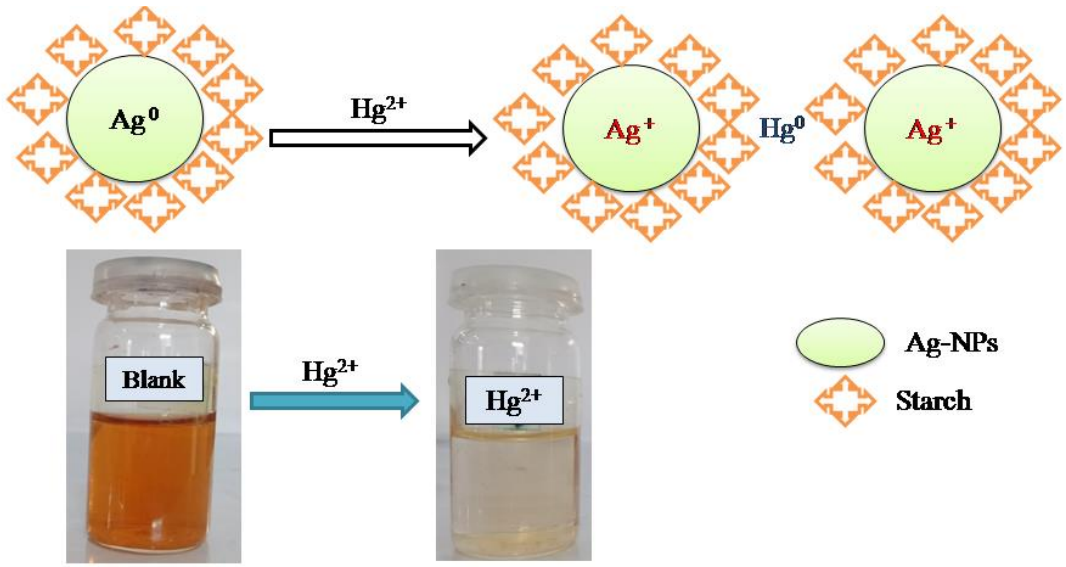

Scheme 4:The proposed the mechanism of the interaction between Starch Coated AgNPs and Hg^{2+} solution.

3.8.1 Screening of heavy metals

NPS behavior towards heavy metals was monitored by UV-Vis spectroscopy. To estimate the detection tendency of AgNPs towards heavy metals, 1mL of AgNPs was mixed with 1mL of aqueous solutions of heavy metals (100ppm), as shown in Table 3.

Table 3: Experimental details for the screening of different heavy metals by AgNPs.

Sample No	Amount of Ag NPs (mg)	Heavy metals	Pollutants Conc (ppm)	Sensing time (min)	Temperature (°C)	pH	Absorption Maxima (a.u.)
01	2	-	100	10	30	5	2.032

02	2	Fe^{2+}	100	10	30	5	1.778
03	2	Cu^{2+}	100	10	30	5	1.917
04	2	Ni^{2+}	100	10	30	5	1.994
05	2	Zn^{2+}	100	10	30	5	1.789
06	2	Pb^{2+}	100	10	30	5	1.881
07	2	Al^{3+}	100	10	30	5	1.827
08	2	Hg^{2+}	100	10	30	5	0.588

The addition of Hg^{2+} resulted in the destruction of AgNPs that was observable as after the addition of Hg^{2+} in AgNPs, the solution suddenly changes its color from reddish yellow to colorless as shown in vials Figure 4(A). UV-Vis spectra reveal broadness and hypochromic shift in the plasmon resonance band. AgNPs dispersion shows utmost absorption intensity at 430 nm which is dismissed by the addition of Hg^{2+}as shown in Figure 4(A).

All other metals including Cu^{2+}, Al^{3+}, Zn^{2+}, Fe^{2+}, and Ni^{2+} did not make any change in the color of AgNPs as well as in the UV spectrum. Hg^{2+} was the only metal that shows clear changes in color and absorption intensity of AgNPs which may be due to redox that can occur between Ag^0 and Hg^{2+}. These results reveal outstanding selectivity over a variety of heavy metals, thus AgNPs have binding sites for Hg^{2+} [37].

3.8.2 Effect of Concentrations of Hg^{2+}

The quantitative estimation of the detection limit of Hg^{2+} ions sensing was studied by altering the concentrations of these Hg^{2+} (1-100 ppm) while keeping the same concentration of AgNPs at the same laboratory circumstances, as shown in Table 4.

Table 4:Experimental details for sensing of different concentrations. of Hg^{2+} by Ag NPs.

Sample No	**Amount of Ag NPs (mg)**	**Hg^{2+} Conc (ppm)**	**Sensing time (min)**	**Temperature (°C)**	**pH**	**Absorption Maxima (a.u.)**
01	2	-	10	30	5	2.722
02	2	1	10	30	5	1.981

03	2	10	10	30	5	1.661
04	2	20	10	30	5	1.610
05	2	30	10	30	5	1.587
06	2	40	10	30	5	1.431
07	2	50	10	30	5	1.406
08	2	60	10	30	5	1.278
09	2	70	10	30	5	1.137
10	2	80	10	30	5	0.831
11	2	90	10	30	5	0.665
12	2	100	10	30	5	0.511

The surface plasmon resonance band of the AgNPs revealed that the mixing of Hg^{2+} ions in the AgNPs solutions produces a steady hypochromic shift in its surface plasmon resonance band at 430 nm. The extent of the shift in the direction of the lower-intensity depends upon the concentrations. of Hg^{2+} ions in that system as shown in Figure 4(B). The decrease in absorbance intensity was observed by an increase in the concentration of Hg^{2+} ions (1 to 100ppm). The value of the linear regression coefficient (R^2) for the system under observation was 0.998 with the detection limit up to 1ppm as shown in Figure 4(C). The same phenomena on AgNPs are also reported in previous research[42].

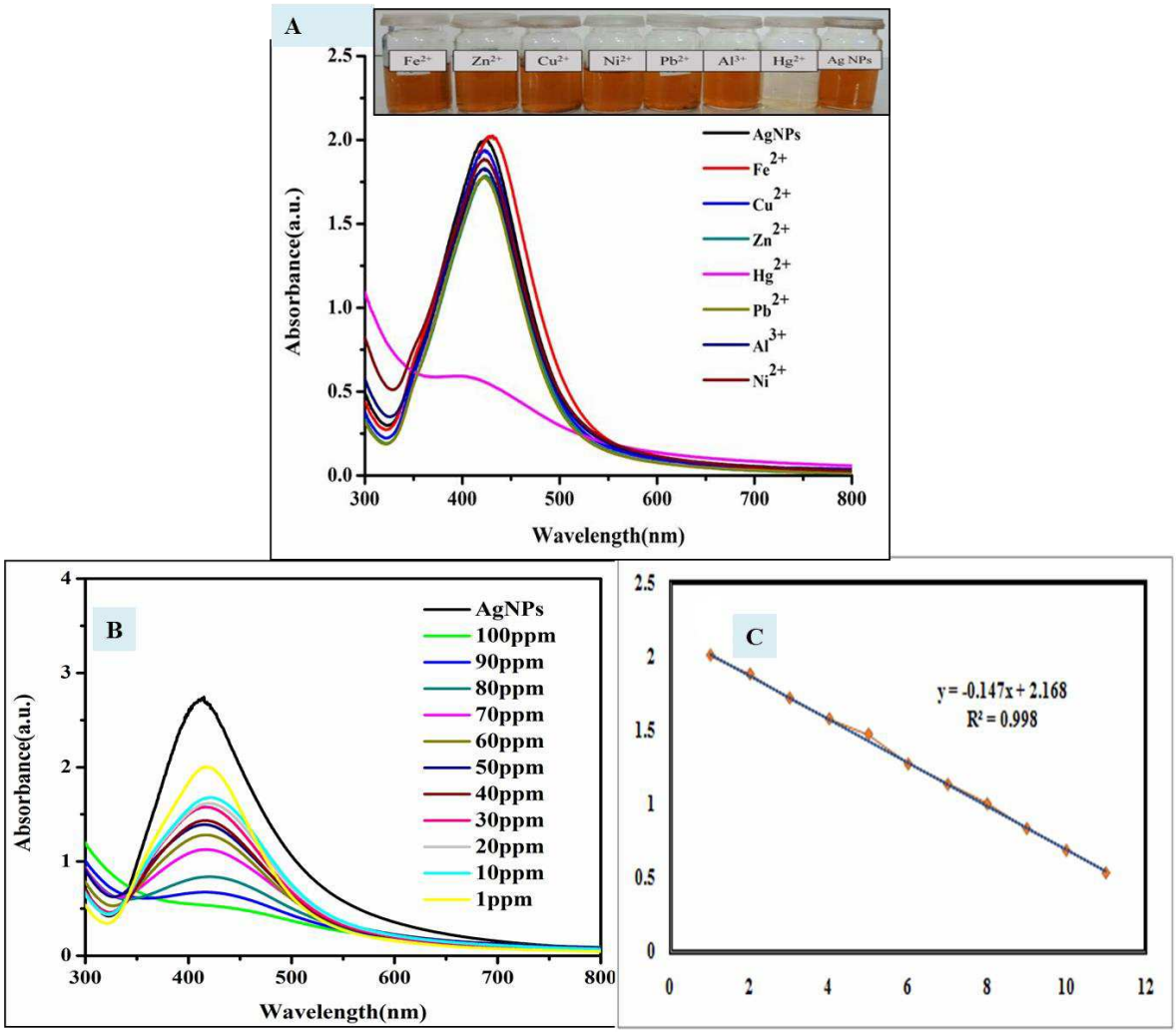

Figure 4 : **(A)** Change in the color of nanoparticles upon addition of Hg^{2+} Photographs & UV absorption spectrum of AgNPs containing 100 ppm of Hg^{2+}, Zn^{2+}, Fe^{2+}, Pb^{2+}, Ni^{2+}, Al^{3+}, Ni^{2+} or Cu^{2+},**(B)** UV spectrum of AgNPs dispersions upon adding various concentrations of Hg^{2+},**(C)** The linear or direct relationship between the absorbance and Hg^{2+} concentrations.

3.8.3 Interference with other metal ions selectivity of the test

To check the selectivity of the above method, 100ppm aqueous solutions of Pb^{2+}, Cu^{2+}, Al^{3+}, Zn^{2+}, Fe^{2+}, $Ni^{2+,}$ and Hg^{2+} were prepared. Keeping the total volume of mixture constant (3 mL), an equal volume of AgNPs, Hg^{2+} (100ppm), and interfering metals solutions were mixed and kept at room temperature to monitor the effect. After a few minutes, the solutions of AgNPs and Hg^{2+} become colorless even in the presence of all metal ions. The hypochromic shift was observed by UV spectrum as shown in Figure 5(A), which indicates that AgNPs can

detect Hg^{2+} ions with high sensitivity even in the existence of the equimolar amount of other interfering cations presence of any other metals[43].

3.8.4 Determination of required stoichiometry of AgNPs and Hg^{2+}

The binding stoichiometry of the AgNPs and $Hg^{2+}$was detected by Job's plot method [44]. Different mole fraction ratios of Hg^{2+} and AgNPs were tested. To monitor the results absorption intensity at 430 nm obtained via UV that was plotted against the molar fraction of Hg^{2+} (100 ppm). The mole fraction of the highest absorption intensity revealed the binding stoichiometry of the compound. 1mL of Hg^{2+}verses 1 mL of AgNPs was present in the sample revealing minimum absorption intensity as shown in Figure 5(B). Result reveals that AgNPs forms a 1:1 complex (AgNPs**:** Hg^{2+}), which means that the best detection of heavy metals occur when there are equal moles of AgNPs and Hg^{2+}[45].

3.8.5 Effect of pH on detection of Hg^{2+}

If circumstances of the detection scheme are altered, then there is a noticeable effect on the sensing of Hg^{2+}. As variation in pH of this system results in aggregation and destabilization of Ag-NPs. 0.1 M KOH and 0.1 M HCl were used to alter the pH of the system from 2-10. UV spectra were recorded for adjusted pH values which indicated AgNPs are stable in basic medium while in acidic medium (pH less than 5) solution become colorless and UV spectra indicate the minimum absorption intensity as shown in Figure 5(C).

The stability of AgNPs in the basic medium is due to an increase in the rate reduction of Ag^{+} ions by OH ions from the base, which results in the increase in the formation of AgNPs that are degraded by Hg^{2+} ions. It means that in basic medium there is a difficulty for Hg^{2+} to degrade the maximum amount of highly stable AgNPs and the reverse was true for acidic pH. The increased stability of AgNPs in alkaline pH might be due to stronger protection of AgNPs by deprotonated OH groups of starch[46].

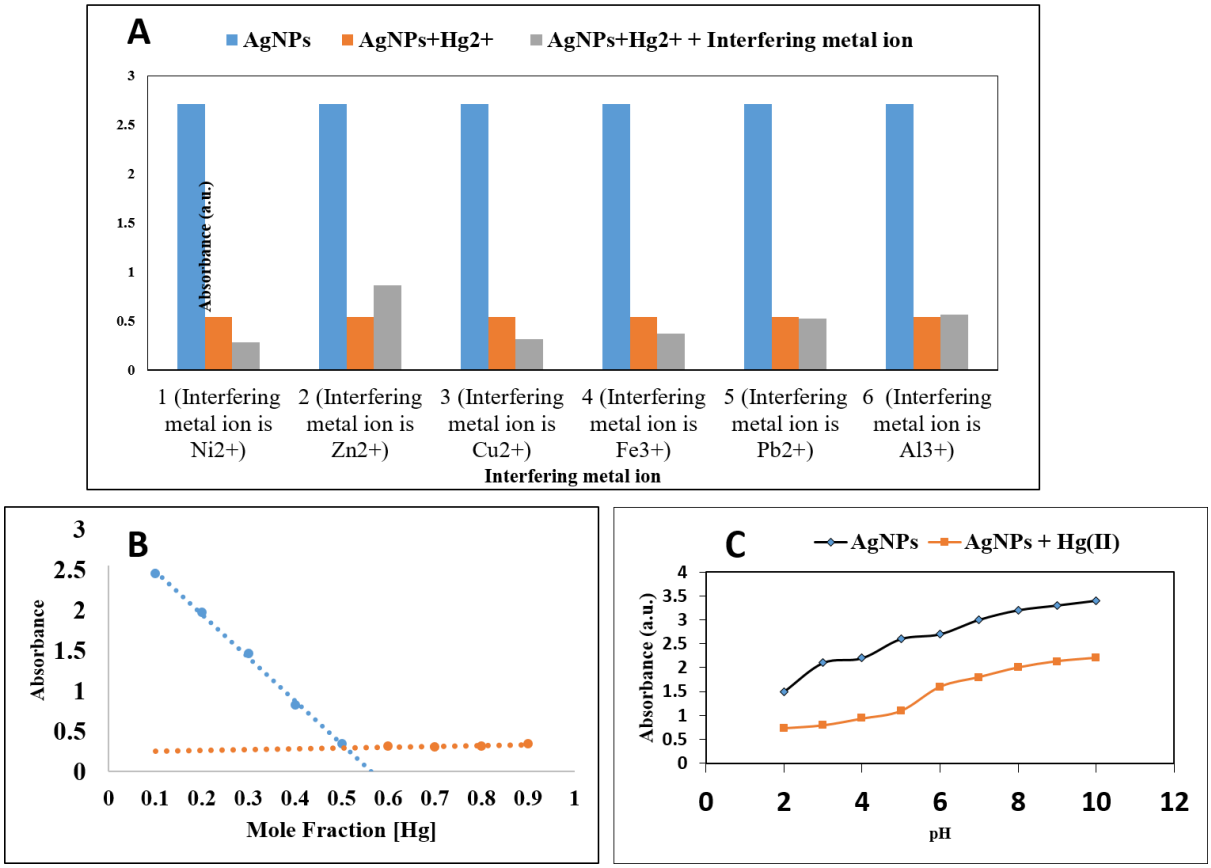

Figure 5: **(A)** Selectivity of Ag-NPs at 430 nm, the blue bar shows the absorption intensity of AgNPs brown bar represents the absorption intensity of AgNPs + Hg^{2+} and green bar represents the absorption intensity of AgNPs + Hg^{2+} in the presence of other metal ions, **(B)** Job's plot curve showing the binding ratio of AgNPs**:** Hg^{2+}, **(C)** Effect of pH on the adsorption of AgNPs in the absence and presence of 100 ppm Hg^{2+} ions.

3.8.6 Spiking in Tap water

Finally, as shown in Table 2 the method we have proposed was applied to real aqueous tap and lake water samples. In order to verify the recovery and accuracy of the proposed method, these samples also spiken with known levels of Hg^{2+}.1 mL Hg^{2+} solution was added in1 mL tap water sample of AgNPs and after some time the solution becomes colorless just like sensing of Hg^{2+} in distilled water. Moreover, UV-visible spectra revealed that the peak become broadened at 430 nm (as

shown above in figure 6) and the same results were observed as shown in distilled water. Hence, AgNPs are found effective for detection of Hg^{2+} in the tap water sample [47]

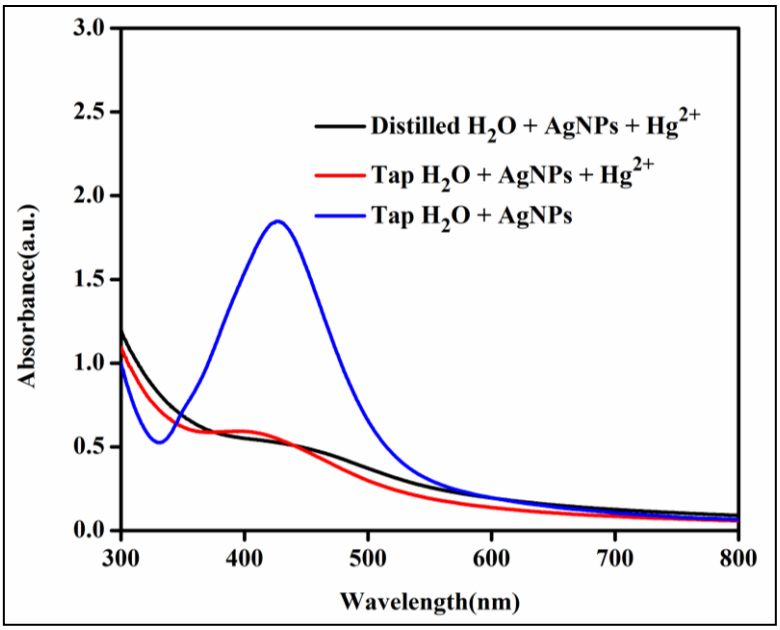

Figure 6:UV Spectrum shows detection of Hg^{2+} in laboratory tap water.

4 Conclusion

In this study, we have developed a facile and green approach for the synthesis of silver nanoparticles by using (5:2:2) by v/v of $AgNO_3$, starch, glucose, and KOH. Characterization of recently synthesized AgNPs was carried out using UV-vis, FT-IR, SEM, and XRD. Moreover, we established the colorimetric as well as SPR detection-based sensing for Hg^{2+} by starch stabilized AgNPs.The strategy is focused on a redox reaction between Starch-AgNP and $Hg^{2+,}$ which results in a shift in color from yellow to colorless nanoparticle dispersions and a decrease in AgNP SPR uptake. Additionally, this approach allows for a wide range of linear detections while avoiding interference from other metal ions. The synthesized AgNPs showed admirable selectivity for Hg^{2+}even in the occurrence of other several heavy metals. That calorimetric chemosensor being useful in laboratory tap water with a detection limit of 1 ppm. In the future, this approach can be modified by using other noble metals such as Au, Pd, and

Pt, etc for the synthesis of nanoparticles which will be used for photophysical and other biological applications.

References

1. D. W. Domaille, E. L. Que and C. J. Chang, *Nature chemical biology*, 2008, **4**, 168.
2. A. R. G. Georgopoulos, MJ Yonone-Lioy, RE Opiekun, PJ Lioy, P, *Journal of Toxicology and Environmental Health Part B: Critical Reviews*, 2001, **4**, 341-394.
3. P. Holmes, K. James and L. Levy, *Science of the total environment*, 2009, **408**, 171-182.
4. R. A. Lavoie, T. D. Jardine, M. M. Chumchal, K. A. Kidd and L. M. Campbell, *Environmental science & technology*, 2013, **47**, 13385-13394.
5. S. Manahan, *Fundamentals of environmental and toxicological chemistry: sustainable science*, CRC press, 2013.
6. M. L. Firdaus, I. Fitriani, S. Wyantuti, Y. W. Hartati, R. Khaydarov, J. A. McAlister, H. Obata and T. Gamo, *Analytical Sciences*, 2017, **33**, 831-837.
7. M. Harada, *Critical reviews in toxicology*, 1995, **25**, 1-24.
8. G. Aragay, J. Pons and A. Merkoçi, *Chemical reviews*, 2011, **111**, 3433-3458.
9. Z. Zhang, A. Tang, S. Liao, P. Chen, Z. Wu, G. Shen and R. Yu, *Biosensors and Bioelectronics*, 2011, **26**, 3320-3324.
10. S. Guha, S. Roy and A. Banerjee, *Langmuir*, 2011, **27**, 13198-13205.
11. M. Ismail, M. Khan, K. Akhtar, M. A. Khan, A. M. Asiri and S. B. Khan, *Physica E: Low-dimensional Systems and Nanostructures*, 2018.
12. L. Fabbrizzi, M. Licchelli, L. Parodi, A. Poggi and A. Taglietti, *Journal of Fluorescence*, 1998, **8**, 263-271.
13. H. A. Mottola and D. Perez-Bendito, *Analytical Chemistry*, 1992, **64**, 407-428.
14. N. Ding, H. Zhao, W. Peng, Y. He, Y. Zhou, L. Yuan and Y. Zhang, *Colloids and Surfaces A: Physicochemical and Engineering Aspects*, 2012, **395**, 161-167.
15. P. Pienpinijtham, X. X. Han, T. Suzuki, C. Thammacharoen, S. Ekgasit and Y. Ozaki, *Physical Chemistry Chemical Physics*, 2012, **14**, 9636-9641.
16. L. S. Walekar, A. H. Gore, P. V. Anbhule, V. Sudarsan, S. R. Patil and G. B. Kolekar, *Analytical Methods*, 2013, **5**, 5501-5507.
17. J. Wang, X. Fang, X. Cui, Y. Zhang, H. Zhao, X. Li and Y. He, *Talanta*, 2018.
18. T. Senapati, D. Senapati, A. K. Singh, Z. Fan, R. Kanchanapally and P. C. Ray, *Chemical communications*, 2011, **47**, 10326-10328.
19. F. Chai, C. Wang, T. Wang, L. Li and Z. Su, *ACS applied materials & interfaces*, 2010, **2**, 1466-1470.
20. Y. Ma, L. Jiang, Y. Mei, R. Song, D. Tian and H. Huang, *Analyst*, 2013, **138**, 5338-5343.
21. G. K. Darbha, A. K. Singh, U. S. Rai, E. Yu, H. Yu and P. Chandra Ray, *Journal of the American Chemical Society*, 2008, **130**, 8038-8043.
22. L.-J. Miao, J.-W. Xin, Z.-Y. Shen, Y.-J. Zhang, H.-Y. Wang and A.-G. Wu, *Sensors and Actuators B: Chemical*, 2013, **176**, 906-912.
23. W. Su, S. Yuan and E. Wang, *Journal of fluorescence*, 2017, **27**, 1871-1875.
24. N. A. Bumagina, E. V. Antina and D. I. Sozonov, *Journal of Luminescence*, 2017, **183**, 315-321.
25. J. T. Huang, X. X. Yang, Q. L. Zeng and J. Wang, *Analyst*, 2013, **138**, 5296-5302.
26. K. Yoosaf, B. I. Ipe, C. H. Suresh and K. G. Thomas, *The Journal of Physical Chemistry C*, 2007, **111**, 12839-12847.
27. H. Li, F. Li, C. Han, Z. Cui, G. Xie and A. Zhang, *Sensors and Actuators B: Chemical*, 2010, **145**, 194-199.
28. D. Karthiga and S. P. Anthony, *RSC Advances*, 2013, **3**, 16765-16774.
29. M. Borbach, W. Stenzel, H. Conrad and A. Bradshaw, *Surface science*, 1997, **377**, 796-801.

30. C. K. Tagad, K. S. Rajdeo, A. Kulkarni, P. More, R. Aiyer and S. Sabharwal, *RSC Advances*, 2014, **4**, 24014-24019.
31. H. Peng, A. Yang and J. Xiong, *Carbohydrate polymers*, 2013, **91**, 348-355.
32. K. Jyoti, M. Baunthiyal and A. Singh, *Journal of Radiation Research and Applied Sciences*, 2016, **9**, 217-227.
33. G. Srirangam and K. P. Rao, *Journal of Chemistry*, 2017, **10**, 46-53.
34. M. Ismail, M. Khan, K. Akhtar, M. A. Khan, A. M. Asiri and S. B. Khan, *Physica E: Low-dimensional Systems and Nanostructures*, 2018, **103**, 367-376.
35. C. K. Tagad, S. R. Dugasani, R. Aiyer, S. Park, A. Kulkarni and S. Sabharwal, *Sensors and Actuators B: Chemical*, 2013, **183**, 144-149.
36. S. M. Meshram, S. R. Bonde, I. R. Gupta, A. K. Gade and M. K. Rai, *IET nanobiotechnology*, 2013, **7**, 28-32.
37. S. Bothra, J. N. Solanki and S. K. Sahoo, *Sensors and Actuators B: Chemical*, 2013, **188**, 937-943.
38. M. Annadhasan and N. Rajendiran, *RSC advances*, 2015, **5**, 94513-94518.
39. Y. Wang, F. Yang and X. Yang, *ACS applied materials & interfaces*, 2010, **2**, 339-342.
40. M. Nidya, M. Umadevi and B. J. Rajkumar, *Spectrochimica Acta Part A: Molecular and Biomolecular Spectroscopy*, 2014, **133**, 265-271.
41. W. Chansuvarn and A. Imyim, *Microchimica Acta*, 2012, **176**, 57-64.
42. L. Li, D. Feng, X. Fang, X. Han and Y. Zhang, *Journal of Nanostructure in Chemistry*, 2014, **4**, 117.
43. U. Khan, A. Niaz, A. Shah, M. I. Zaman, M. A. Zia, F. J. Iftikhar, J. Nisar, M. N. Ahmed, M. S. Akhter and A. H. Shah, *New Journal of Chemistry*, 2018, **42**, 528-534.
44. K. Shah, N. ul Ain, F. Ahmed, I. Anis and M. R. Shah, *Sensors and Actuators B: Chemical*, 2017, **249**, 515-522.
45. H. N. Kim, W. X. Ren, J. S. Kim and J. Yoon, *Chemical Society Reviews*, 2012, **41**, 3210-3244.
46. V. V. Kumar, S. Anbarasan, L. R. Christena, N. SaiSubramanian and S. P. Anthony, *Spectrochimica Acta Part A: Molecular and Biomolecular Spectroscopy*, 2014, **129**, 35-42.
47. Y. Luo, S. Shen, J. Luo, X. Wang and R. Sun, *Nanoscale*, 2015, **7**, 690-700.